metals

MDPI

Article

Biocompatibility and Cellular Behavior of TiNbTa Alloy with Adapted Rigidity for the Replacement of Bone Tissue

Mercè Giner [1,*], Ernesto Chicardi [2,*], Alzenira de Fátima Costa [3], Laura Santana [2], María Ángeles Vázquez-Gámez [4], Cristina García-Garrido [5], Miguel Angel Colmenero [3], Francisco Jesús Olmo-Montes [3], Yadir Torres [2] and María José Montoya-García [4]

1 Departamento de Citología e Histología Normal y Patológica, Universidad de Sevilla, 41009 Sevilla, Spain
2 Departamento de Ingeniería y Ciencia de los Materiales y del Transporte, Escuela Politécnica Superior, Calle Virgen de África 7, 41011 Sevilla, Spain; lausanroc@alum.us.es (L.S.); ytorres@us.es (Y.T.)
3 Servicio de Medicina Interna, HUV Macarena, Avda Sánchez Pizjuán s/n, 41009 Sevilla, Spain; alzenira.costa@juntadeandalucia.es (A.d.F.C.); mangel.colmenero.sspa@juntadeandalucia.es (M.A.C.); franciscoj.olmo.sspa@juntadeandalucia.es (F.J.O.-M.)
4 Departamento de Medicina, Universidad de Sevilla, Avda. Dr. Fedriani s/n, 41009 Sevilla, Spain; mavazquez@us.es (M.Á.V.-G.); pmontoya@us.es (M.J.M.-G.)
5 Instituto Andaluz del Patrimonio Histórico (IAPH), Camino de los Descubrimientos s/n., 41092 Sevilla, Spain; cristina.g.garrido@juntadeandalucia.es
* Correspondence: mginer@us.es (M.G.); echicardi@us.es (E.C.)

Abstract: In this work, the mechanical and bio-functional behavior of a TiNbTa alloy is evaluated as a potential prosthetic biomaterial used for cortical bone replacement. The results are compared with the reference Ti c.p. used as biomaterials for bone-replacement implants. The estimated mechanical behavior for TiNbTa foams was also compared with the experimental Ti c.p. foams fabricated by the authors in previous studies. A TiNbTa alloy with a 20–30% porosity could be a candidate for the replacement of cortical bone, while levels of 80% would allow the manufacture of implants for the replacement of trabecular bone tissue. Regarding biocompatibility, in vitro TiNbTa, cellular responses (osteoblast adhesion and proliferation) were compared with cell growth in Ti c.p. samples. Cell adhesion (presence of filopodia) and propagation were promoted. The TiNbTa samples had a bioactive response similar to that of Ti c.p. However, TiNbTa samples show a better balance of bio-functional behavior (promoting osseointegration) and biomechanical behavior (solving the stress-shielding phenomenon and guaranteeing mechanical resistance).

Keywords: prosthetic material; TiNbTa; osteoblastic cells; cellular adhesion; porous titanium; mechanical behavior

Citation: Giner, M.; Chicardi, E.; Costa, A.d.F.; Santana, L.; Vázquez-Gámez, M.Á.; García-Garrido, C.; Colmenero, M.A.; Olmo-Montes, F.J.; Torres, Y.; Montoya-García, M.J. Biocompatibility and Cellular Behavior of TiNbTa Alloy with Adapted Rigidity for the Replacement of Bone Tissue. *Metals* **2021**, *11*, 130. https://doi.org/10.3390/met11010130

Received: 11 December 2020
Accepted: 2 January 2021
Published: 11 January 2021

1. Introduction

The increase in life expectancy and population aging generate increasing demand for the repair of worn or degenerated tissues, for the restoration of organ functions, and esthetic restoration. Among these, bone tissue is one of the most popular [1]. Replacement medical systems require materials with essential properties that enable interaction with bone. These materials must be resistant to corrosion and wear and have high hardness and ductility. The proper selection of the biomaterial is the key factor for the long-term success of the implant. Hitherto, titanium has been the material of choice for intraosseous applications due to its excellent osseointegration capacity, biocompatibility, high resistance to corrosion, a modulus of elasticity compatible with that of bone, and very good tolerance for soft tissues [2,3]. Its anchorage to bone tissue is possible thanks to the oxide layer formed in the material when passivated [4].

Pure commercial titanium (Ti c.p.) and the Ti-6Al-4 V alloy are currently largely used for bone implants. However, both elements present a high elastic modulus, E, (100–112 GPa) compared to the elastic modulus of cortical bone (15–25 GPa) and trabecular bone (less

than 1 GPa) [4,5] which produces the effect of Stress-Shielding [6]. This phenomenon arises since the stiffness of the bone-implant material is greater than the stiffness of the bone itself, which causes the whole load to fall on the bone implant. This imbalance in mechanical loads influences bone remodeling and increases bone formation in the heaviest areas and decreases it in areas with no gravitation.

The areas with fewer stimuli present lower bone density, which favors premature fractures and/or the loosening of the implant [7]. Currently, research is aimed at reducing the elastic modulus of the material. One approach to solve this issue involves the design and manufacture of porous metallic biomaterials that combine the low stiffness of porous structures [8,9]. It should also be borne in mind that the higher the porosity, the lower the mechanical strength and wear resistance of the porous structure. Another approach to address this specific issue in titanium alloys is to reduce the stiffness by designing alloys with low Young's modulus and the high strength of metallic alloys [10]. Two generations of Ti alloys have been developed for biomedical applications [3,11]. The first generation presents both α and (α + β) phases, while the second generation of Ti alloys is called the β-phase Ti-based alloys [10–12]. In the first, depending on the alloying elements, a cytotoxic effect must be taken into account [13]. For example, Ti, Zr, Ta, and Pd are elements of low cytotoxicity [13], while Al, V, Ni, and Co have been reported as cytotoxic [13]. On the other hand, the other generation (β-phase Ti-based alloys) have been preferred mainly due to their lower elastic modulus [14]. In these, the presence of β-phase is promoted by incorporating β-stabilizing elements, such as Pd, Ni, Mo, Ta, V, Mn, and Nb [15]. Several authors have identified the biological impact of a number of those elements on human health: Ti, Nb, Ta, Mn, Zr, and Ru are reported to have been found to exhibit the best bio-functional behavior [13,14], while the Ta, Nb, and Zr decrease the elastic modulus of this type of alloys and increase their mechanical strength [13–20]. Novel beta alloys based on this concept are the commercial TLM alloy (Ti-25Nb-3Zr-3Mo-2Sn) [21], the quaternary Ti-Nb-Sn-Cr [22], Ti-Nb-Zr-Cr [23] and Ti-Nb-Zr-Ta alloys systems [24], among others [3,25]. All of them showed elastic modulus still higher than the cortical bone tissue (minimum value reached around 45 GPa).

Specifically, Chicardi et al. [26,27] have recently fabricated a (β + γ)-TiNbTa material (bcc and innovative structures for Ti alloys, for α and β phases, respectively), with physico-chemical properties more similar to those of the bones and with Young's modulus more similar to cortical bone. In particular, this TiNbTa material has been shown to decrease the elastic modulus (49 + 3 GPa) and to maintain excellent yield strength (σy > 1860 MPa) with expected high biocompatibility [28], which places it among the ideal materials to prevent the *Stress-Shielding* phenomena by the two aforementioned synergic ways to solve this issue: (a) the formation of partial β (bcc) phase with low stiffness instead of the elimination of the α- phase, with high stiffness and (b) the introduction of porosity to further decrease its elastic modulus to approximate it to the cortical and/or trabecular bone without the inadmissible sudden drop in the yield strength.

However, the characterization of this material is still incomplete as regards its validation for use as a metallic biomaterial for bone grafts or implants, which constitutes the main objective of this work. It remains necessary to compare this material with the widely employed Ti c.p. and its foams by evaluating the potential mechanical properties of TiNbTa foams, the osseointegration capacity of this new TiNbTa-based biomaterial, and by determining its cytotoxicity, adhesion capacity, proliferation, and differentiation on osteoblastic cells.

2. Materials and Methods

2.1. Development and Mechanical Characterization of the TiNbTa Potential Prosthetic Biomaterial

The new potential TiNbTa material was developed from the elemental Ti, Nb, and Ta powder transition metals as raw materials using a Powder Metallurgy route, including the mechanical alloying (MA) and subsequent consolidation of the as-synthesized TiNbTa alloy by spark plasma sintering (SPS). A schema of the route used is displayed in Figure 1.

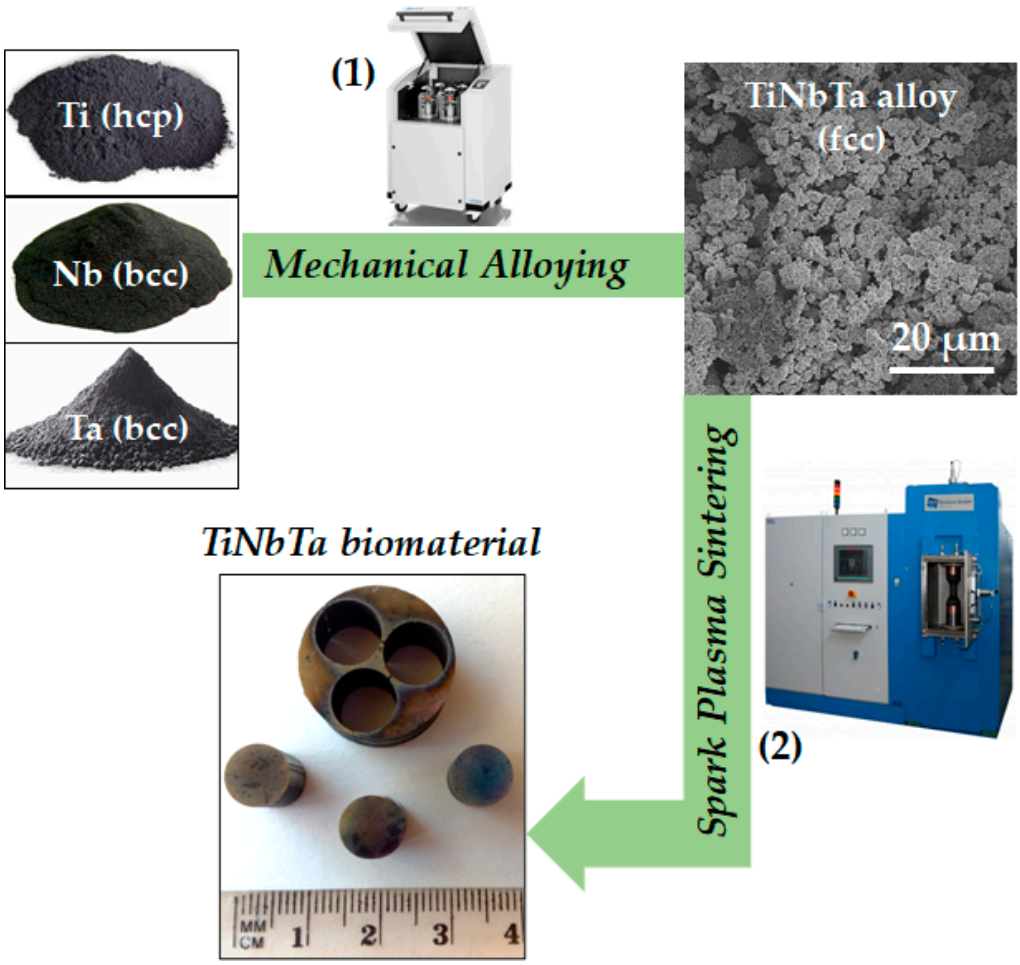

Figure 1. Schema of the powder metallurgy route used for the development of the new potential prosthetic TiNbTa material, showing the evolution of the material from raw elements (Ti, Nb, and Ta) to the synthesized TiNbTa alloy, and, finally, to the fabricated potential prosthetic TiNbTa biomaterial. (1) Image of the PM400 planetary ball mill, courtesy of Retsch. (2) Image of the HPD 25 spark plasma sintering (SPS) device, courtesy of FCT Systeme GmbH.

Specifically, the Ti, Nb, and Ta powders, with particle size < 325 mesh and purity > 99.6%, were supplied by NOAH tech, San Antonio, TX, USA. Therefore, 50 g of the mix of powders, with a nominal composition of 57% of Ti, 30% of Nb, and 13% of Ta, were milled in a PM400 planetary ball mill supplied by Retsch GmbH. The optimized milling conditions were a spinning rate of 250 rpm; a ball-to-powder ratio (BPR) of 10:1; yttria-stabilized zirconia (YSZ) balls and vial (500 mL in volume); an Ar atmosphere to prevent the oxidation of metals during milling; and 60 h of milling time.

The as-synthesized TiNbTa alloy was consolidated with cylindrical geometry (20 mm in diameter and 10 mm in height) by spark plasma sintering (SPS) using a commercial HPD 25 spark plasma sintering (SPS) device, fabricated by FCT Systeme GmbH. The sintering conditions included a dwell temperature of 1400 °C, a heating rate of 500 °C/min, no dwell time, and a free in-air cooling rate (calculated as approximately 700 °C/min). An in-depth description of the processing route can be found elsewhere [27].

The newly developed TiNbTa potential prosthetic material was microstructurally characterized [26], and the mechanical behavior, biocompatibility, and osseointegration were studied in this work. For mechanical behavior, two key parameters were used for a prosthetic biomaterial performance: the elastic modulus (E) and the yield strength (σy). These were determined from a stress–strain curve obtained in a uniaxial compression test. This test was carried out on five reproduced TiNbTa specimens in a universal mechanical testing machine (Model 6025, by Instron) and, in accordance with the ASTM E9-09 standard,

with a displacement rate of 0.05 mm/min and a maximum load of 100 kN. The specimens were tested, of 8 mm in diameter and 10 mm in height, in accordance with the "short solid cylindrical specimens" in the ASTM E9-09, were machined from the aforementioned cylinders (20 mm in diameter and 10 mm in height, see Figure 1) by the wire electro-erosion process in electrical discharge machining (EDM).

On the other hand, the elastic modulus (E) and the yield strength (σy) for porous TiNbTa materials, with porosities from 10 up to 90 vol %, were estimated from the E and σy values corresponding to the fully dense TiNbTa presented and the empirical Mondal equation [29].

2.2. In Vitro Cell Experiments

MC3T3E1, a murine pre-osteoblast cell line (CRL-2593, from ATCC), was utilized to analyze the TiNbTa effect on cell metabolism and viability during the cell adhesion and proliferation process.

The different techniques employed to evaluate cellular response are described in Figure 2.

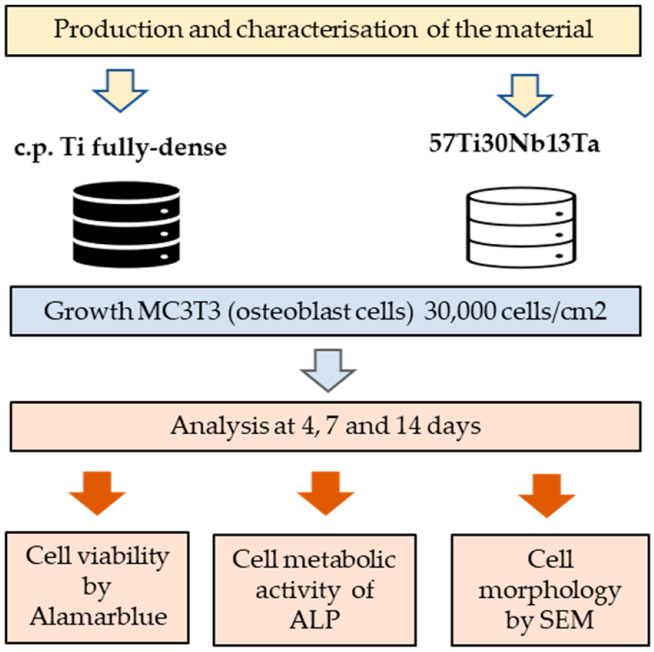

Figure 2. Diagram of in vitro experimental design. Osteoblast cell line (MC3T3E1) was used to analyze the biological response to fully dense Ti c.p. vs. TiNbTa samples.

2.3. Cell Culture

MC3T3E1, a murine pre-osteoblast cell line (CRL-2593, from ATCC), was employed to analyze the TiNbTa effect on cell metabolism and viability during the cell adhesion and proliferation process. Routine passaging of the cell line was performed on 25 cm^2 flasks with minimum essential medium (MEM), containing 10% fetal bovine serum plus antibiotics (100 U/mL penicillin and 100 mg/mL streptomycin sulfate) (Invitrogen). Sample discs were autoclaved at 121 °C for 30 min and were then placed onto a 24-well plate. Osteoblast cells were seeded at a cell density of 30,000 cells/cm^2 per sample and in 800 µL of prewarmed culture medium. Plates were kept at 37 °C in a humidified 5% CO^2 atmosphere, and as a control, triplicate blank TCP (tissue culture plastic) and fully dense pure titanium discs were employed as negative and positive controls on the same plate for each time of period.

At 48 h of osteoblast cultured on TiNbTa and fully dense Ti c.p. samples, the cell media was changed to osteogenic media (α-MEM medium) supplemented with 10 mM of ascorbic acid (Merck, Germany) and 50 µg/mL of β-glycerophosphate (StemCell Technologies,

Canada). The in vitro cell experiments were carried out at 4, 7, and 14 days of cell incubation in which the samples were transferred onto a new 24-well plate to prevent counting non-attached or attached cells on the well plate.

2.4. Cell Viability and Proliferation Assay

Cell proliferation and viability tests were evaluated using alamarBlue® reagent (Invitrogen). In accordance with the manufacturer's protocol, new fresh media (800 µL) and 80 µL of alamarBlue® reagent were added, and the plate was incubated for 1 h 30 min at 37 °C in dark conditions. The absorbance at 570 nm (TECAN, Infinity 200 Pro) was subsequently recorded.

2.5. Cell Differentiation by Alkaline Phosphatase (ALP) Evaluation

MC3T3 differentiation levels were evaluated through alkaline phosphatase (ALP) activity, using the alkaline phosphatase assay kit (Colorimetric) (Abcam ab83369, UK). The assay was performed on days 4, 7, and 14 in triplicate according to the manufacturer's protocol. The absorbance at 405 nm of 4-nitrophenol was measured in a 96-well microplate reader. Data are expressed as µmol/min/mL of pNPP.

2.6. Cell Morphology

Scanning electron microscopy (SEM) was employed to evaluate cell behavior at 4, 7, and 14 days. The samples were fixed in 10% formalin, which was followed by a dehydration step with ethanolic solutions and then coated by gold-coating using a sputter coater (Pelco 91000, Ted Pella, Redding, CA, USA). The images were obtained using a Jeol JSM-6330 F scanning electron microscope (JEOL, Tokyo, Japan) with an acceleration voltage of 10 kV.

2.7. Statistical Analysis

All experiments were performed in triplicate in order to ensure reproducibility. The results were expressed in terms of the mean and standard deviation to perform two-way ANOVA, followed by Tukey's posttest using SPSS v.22.0 for Windows. The significance level was considered at p values of $p < 0.05$ (*) and $p < 0.01$ (**).

3. Results and Discussion

The following section presents the results related to the mechanical and cellular behavior of the TiNbTa-based potential prosthetic biomaterial developed, comparing it with Ti c.p. (porous and fully dense). Therefore, the study of cellular response correlated to the mechanical properties of TiNbTa could be assessed.

3.1. Mechanical Behavior of the TiNbTa Potential Prosthetic Biomaterial and Comparison with Actual Biomaterials

The strain-stress curve obtained for the fully dense TiNbTa specimen from the compression tests gave elastic modulus (E) and yield strength (σy) values of 49 ± 3 GPa and 1860 ± 20 MPa, respectively (Table 1), as previously reported. This mechanical behavior is, a priori, interesting for the use of this material as a prosthetic biomaterial for bone tissue replacement. Not in vain, although the elastic modulus value obtained is similar, as an example, to another beta (bcc) Ti alloy already developed by Zhang et al. [30], concretely, the accepted as biomaterial Ti24Nb4Zr8Sn alloy (E = 53 GPa), the yield strength is much higher in comparison with this alloy (σy ~800 MPa). In addition, although the elastic modulus seems to remain elevated in comparison with the cortical (15–25 GPa) and cancellous (less than 1 GPa) bone tissues [31], the high yield strength value is shown grants this material the opportunity to adjust the elastic modulus value to both cortical and cancellous bone by the introduction of porosity without an impermissible decrease in yield strength. To this end, both key mechanical properties for metallic biomaterials for implants were estimated for hypothetical porous TiNbTa materials from the values corresponding to the fully dense TiNbTa presented and the empirical Mondal equation [29].

Furthermore, these determined values were compared with the various E and σy values for the titanium foams of previously published biomaterials that were fabricated by the space-holder powder metallurgy route and the fully dense Ti c.p. used as biomaterials for implants. Thus, both sets of serial data (E and σy for the TiNbTa and the fully dense Ti c.p. and foam materials) are compared in Figure 3. It can be observed how it is possible to reach Young's modulus corresponding to the cortical and even to the cancellous bone tissue through the introduction of a range of 20–30 vol % and more than 80 vol % of porosity, respectively, on the two materials, that is, for the new TiNbTa material and the currently used Ti c.p. (Figure 3a). However, regarding the damage to the yield strength for both materials, the introduction of porosity in the TiNbTa materials enables a higher value of σy to remain in comparison with the Ti c.p. (Figure 3b) and significantly higher than that of the cortical bone (227 MPa). This is a positive aspect that prevents or delays the plastic deformation of the TiNbTa in comparison with Ti c.p. for the same Young's modulus.

Table 1. Total volumetric porosity (p), elastic modulus (E), and yield strength (σy) for (a) the developed fully dense TiNbTa material and the corresponding TiNbTa foams, with volumetric porosities from 10 to 70 vol %, calculated by the Mondal equation [29]; (b) the Ti foams developed by the space-holder, also with volumetric porosities from 10 to 70 vol % and marked as "a" or "b" when NaCl or NH_4HCO_3 was used as the space-holder, respectively; (c) commercial Ti c.p., commercial Ti6Al4V [4]; (d) cortical and cancellous bone tissues [5,31].

Specimen	Total Porosity (p,%)	E (GPa)	σ_y (MPa)
TiNbTa_0	0	48.0	1860
TiNbTa_10	10	35.0	1357
TiNbTa_20	20	25.2	976
TiNbTa_30	30	17.7	685
TiNbTa_40	40	12.0	465
TiNbTa_50	50	7.7	300
TiNbTa_60	60	4.6	179
TiNbTa_70	70	2.4	95
TiNbTa_80	80	1.0	40
TiNbTa_90	90	0.2	9
Ti_60a	57	8.1	16
Ti_70a	64	3.5	42
Ti_30b	28	15.9	389
Ti_40b	38	5.8	272
Ti_50b	45	8.5	192
Ti_60b	55	3.7	112
Ti_70b	63	4.6	57
Ti c.p.	0	105	480
Ti6Al4V	0	110	870
Cortical bone tissue	~0	[15–25]	[80–200] *
Cancellous bone tissue	>30	<1	[1–9] *

* ultimate tensile strength (σUTS).

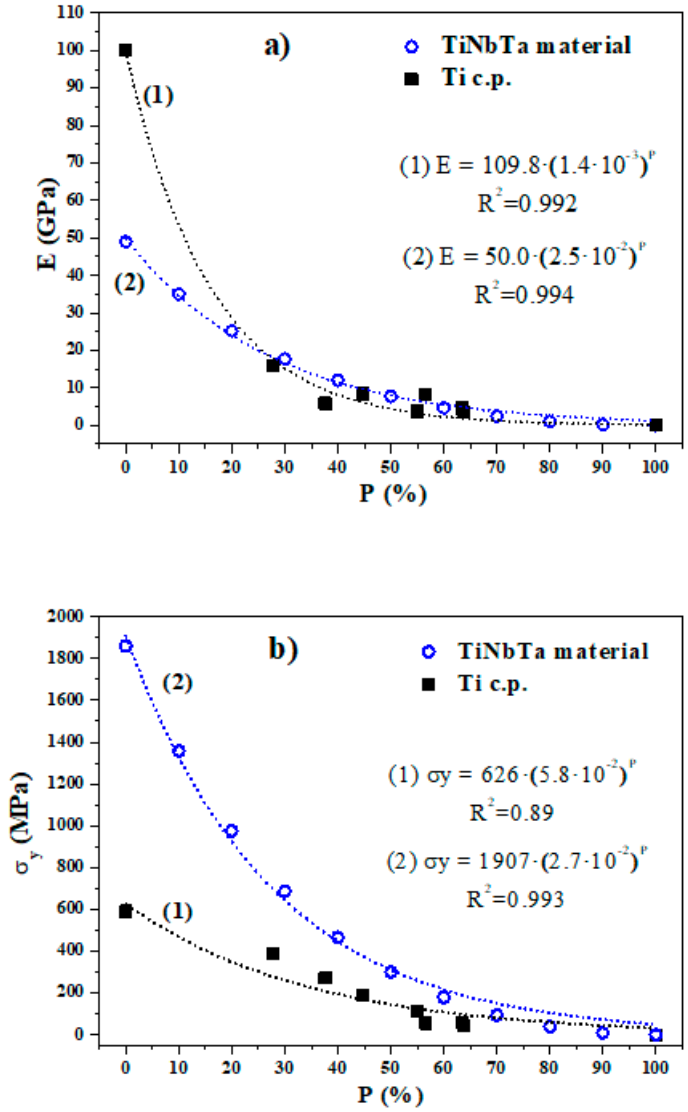

Figure 3. (**a**) Elastic modulus (E) and (**b**) yield strength (σy) for both TiNbTa material (○) and Ti c.p. (ν) foams in terms of the porosity introduced in the specimen. Note that the values for TiNbTa are determined by the Mondal equation, except the experimental values obtained from the compression test for fully dense TiNbTa, and that the values for Ti c.p. are experimentally obtained in previous work. The equations displayed correspond to the best fit (exponential curves) to the serial data.

Subsequently, Figure 4 shows the double logarithmic E-σy curves for the Ti c.p. and TiNbTa fully dense and foam materials. Moreover, the same values for the Ti6Al4V biomaterial and the interval values for the cortical and cancellous bone tissues were introduced for comparison purposes. It should be borne in mind that the main objective of this linearized figure is to maximize the index σy/E, that is, minimize the E and, consequently, diminish the potential detrimental "Stress-Shielding" phenomena of a possible implant fabricated with these materials, but with a maximization of the yield strength (σy), thereby avoiding the plastic deformation of the implant. Thus, after linearization, the index σy/E = C evolves to the line equation log σy = log (E) + log C. Using a line with a slope equal to 1 (marked in Figure 4 as a dotted line), it is possible to maximize the ordinate at the origin (log (C)), and, therefore the index C = σy/E, as desired. With this reasoning, the specimens that optimize this index σy/E for the cortical bone are those named either TiNbTa_20 or TiNbTa_30, that is, the TiNbTa foams with 20 and 30 vol % of porosity, respectively. This assertion is in concordance with the optimized specimens selected attending to the relationship porosity-E and porosity-(σy) (TiNbTa_20 and TiNbTa_30) as determined in

Figure 3. However, a higher amount of porosity (10% more) could be introduced for TiNbTa_30, thereby enabling improvements in the cells' ingrowth to the implant without any detrimental effect on mechanical behavior; these last specimens could be accepted as the optimized materials for cortical bone tissue replacement. Furthermore, for both specimens, the yield strength obtained is sufficient in comparison with the maximum yield strength of the cortical bone tissue. It should be taken into consideration that, although the Ti_40b seems to have a higher $\sigma_y/E = C$ than the cortical bone, its lower E value in comparison with the cortical bone could affect the mechanical behavior of the implant with a non-acceptable elastic deformation.

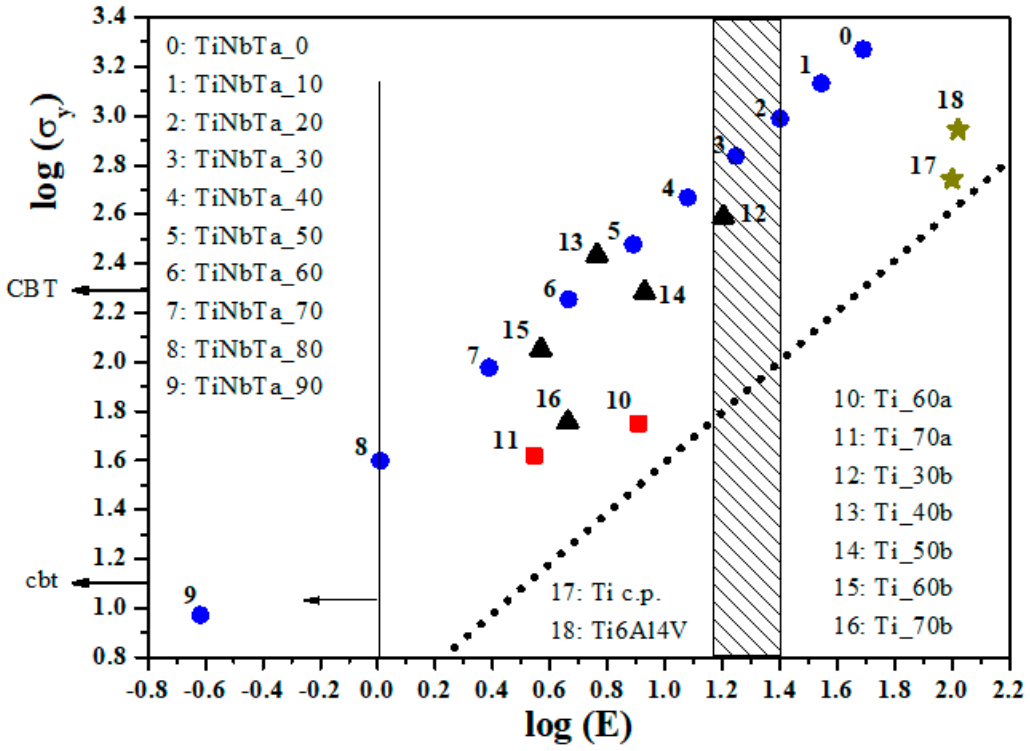

Figure 4. Comparison between elastic modulus (E) and yield strength (σ_y) for: (**a**) the developed fully dense TiNbTa material and the corresponding porous TiNbTa (•); (**b**) Ti foams (fabricated by the space-holder, using sodium chloride (NaCl) (v), and ammonium bicarbonate (NH_4HCO_3) (▲); (**c**) commercial Ti c.p. (number 17) and commercial Ti6Al4V (number 18). The striped column marks the limits between the interval E values for cortical bone tissues. In turn, the E values for cancellous bones (less than 1 GPa) are marked with the continuous line and the arrow to the left. CBT and cbt: maximum value of yield strength for cortical (CBT) and cancellous (cbt) bone tissues, respectively. In addition, for comparison purposes, the dotted line marks the slope line equal to 1 to observe the specimens that maximize the index σ_y/E.

On the other hand, related to the selection of an optimal material to replace the cancellous bone tissue, only specimen TiNbTa_80 accomplishes the requirements (<1 GPa and 9 MPa for E and σ_y for the cancellous bone tissue). Specifically, Young's modulus is equal to 1 GPa, and 40 MPa of yield strength was calculated (see Table 1). However, the high level of porosity (80 vol %) could complicate the manufacturing of this potential biomaterial to replace the cancellous bone by means of powder metallurgy routes.

3.2. Biocompatibility of the TiNbTa Potential Prosthetic Biomaterial

MC3T3 cells were seeded on TiNbTa and Ti c.p. substrates to evaluate proliferation, metabolism cells, and cell adhesion for 4, 7, and 14 days. Cell cultures in both samples had similar cell growth. At 7 days of growth, the cells present a columnar and basophilic morphology compatible with the onset of differentiation.

Figure 5 shows the viability of the cell line as a function of the cell growth time (4, 7, and 14 days) on the Ti c.p. and TiNbTa. At 4 and 7 days of culture, the cell viability in the TiNbTa discs is similar to that of the Ti c.p., while at 14 days, a slight decrease in viability in the TiNbTa samples and an increase in the Ti c.p. can be observed, although without significant differences. Significant differences appear between days 7 and 14 of the cells grown on the surface of TiNbTa, in which there is a decrease in proliferation at 14 days. This decrease is to be expected since the differentiation begins on osteoblastic cells, and when differentiating, they lose their proliferation capacity.

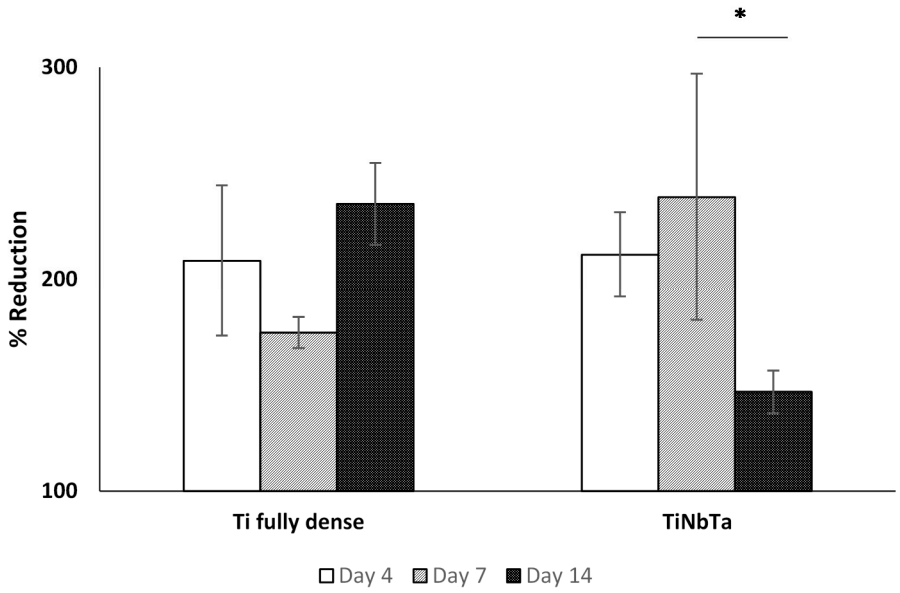

Figure 5. Cell viability of cultured cells from fully dense Ti or TiNbTa at 4, 7, and 14 days of cell growth. The results are presented as mean ± standard deviation, * $p < 0.05$.

Currently, titanium constitutes the most used material in biomedical implants [19], mainly commercially pure titanium and the alloy with titanium, aluminum, and vanadium (Ti-6Al-4 V). Despite its good biocompatibility and resistance to corrosion, there are still certain limitations from the clinical point of view due to complications, such as the toxicity of vanadium and aluminum and the stress-shielding effect [12,20].

Previous studies carried out in fibroblasts demonstrated that the TiNbZrTa alloy does not have a direct or indirect cytotoxic effect on these cells [32], which indicates that it is a safe alloy for use as a biomaterial. It has been shown that Nb and Ta, in addition to not being toxic substances, also inhibit the release of metal ions through the formation of an oxide layer formed by TiO_2 and Nb_2O_5 on the surface of the material [33–35], and this increases their resistance to corrosion [26]. These studies indicate that the use of the TiNbZrTa alloy in the biomedical area is highly recommended due to the low release of metals in vitro and a low elastic modulus, which is very beneficial, especially for long-term implants [36].

Several preliminary studies have shown that the physical and chemical characteristics of the biomaterial surface directly or indirectly affect the adhesion, proliferation, differentiation, and interaction with the cell and consequently the cell environment in the various stages of differentiation in response to the surface of the material [37]. Our assays demonstrated cell viability and proliferation on every surface studied. No differences in cell viability were observed between the two types of the disc at four days of culture. However, in the samples cultured on the TiNbTa discs, a slight increase in cell viability at seven days was observed, but without significant differences (Figure 5). These results are similar to those previously published by Qian Wang et al. [38] in studies carried out on osteoblasts cultured on porous Ta, and they also agree with the results published by Donato et al. [32] in studies carried out on fibroblast cultures.

In all cases, the viability percentage is always greater than 150%. A toxic effect is considered when the viability is less than 75%; therefore, with the results obtained, it can be deduced that cell culture is viable throughout the entire duration of the culture in all conditions, fully agreeing with previous results published by Qian Wang et al. [38] and Shimko et al. [39].

Another important consideration involves the levels of alkaline phosphatase (ALP) secreted by osteoblasts during the osseointegration process. ALP is a glycoprotein abundantly expressed in the extracellular matrix and is considered a marker in the initial stage of osteogenic differentiation [40,41]. Several studies relate the activity of alkaline phosphatase with the process of cell differentiation, together with other specific proteins, such as osteocalcin, osteopontin, osteonectin, and type I collagen [42,43].

Figure 6 represents the alkaline phosphatase (ALP) activity values in MC3T3 cell cultures at 4, 7, and 14 days. In TiNbTa discs, a decrease in activity is also observed with the culture time, and there is a significant difference between days 4 and 7, and also between days 7 and 14 of culture ($p < 0.001$). In Ti c.p. discs, the results obtained show a decrease in enzyme activity, whereby the difference found between days 4 and 7 are statistically significant ($p < 0.05$). In both conditions, at 4 days, the maximum enzymatic activity is obtained since there is a greater proliferation and cell growth as the viability values corroborate. From day 7, the cells present a more differentiated phenotype as can be observed in the SEM images, and the ALP activity decreases.

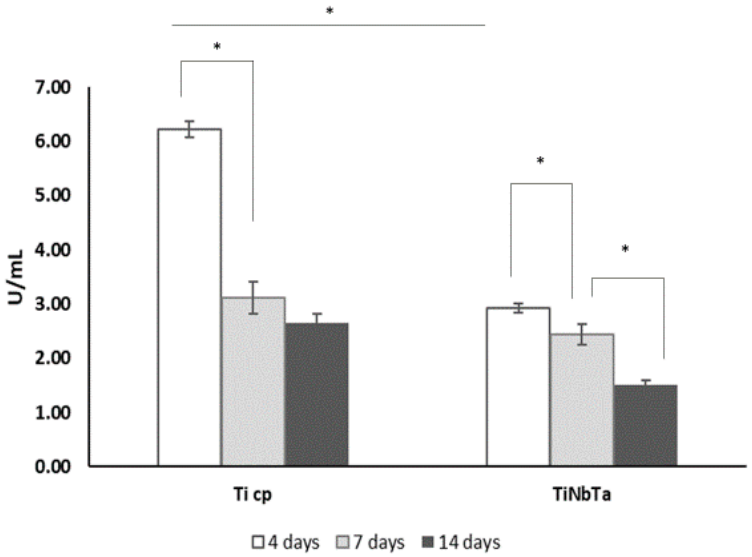

Figure 6. Alkaline phosphatase activity in cell growth on discs of fully dense Ti or TiNbTa at 4, 7, and 14 days. * $p < 0.05$.

According to these results, both discs stimulate cell differentiation. The maximum levels of ALP activity observed at four days of culture suggest a high level of cell differentiation. The decrease in the levels of this protein observed after seven days are compatible with the beginning of the cell differentiation process to a mineralizing phenotype, which supports the fact that ALP is indeed an early marker of cell differentiation. Similar results were observed in other studies in which alkaline phosphatase activity was analyzed in osteoblast cell culture. Boyan et al. [44] also observed a decrease in alkaline phosphatase activity in cells grown on rough surfaces on analyzing Saos2 (Osteogenic Sarcoma) cells, a cell line similar to human osteoblasts.

A preliminary study was conducted to study cell morphology and adhesion on TiNbTa study material compared to growth in Ti c.p. To this end, the samples of both types of discs at 4, 7, and 14 days of culture were visualized. At four days, small cell clusters were observed on both types of surface and of similar density. At seven days, the images demonstrated a monolayer growth on the entire surface of the disc; these results were

similar for both materials. In addition, we can begin to observe small morphological changes in the cells grown on Ti cp; they are more stellate cells, while in the alloy, they maintain the fibroblastic shape. Cell-cell and cell-biomaterial junctions were also observed. The cells adhere through filopodia (fine cell projections, yellow arrow) and lamellipodia (wider extensions, yellow asterisk), thus demonstrating the connection of the cells with the biomaterial. At 14 days, the presence of small hexagonal-structure vesicles (red asterisk) can already be observed, which suggests possible nucleation of hydroxyapatite on the cell surface, as an indication of the start of the development of the mineralization process, and a clear difference is seen between the morphology of the cells grown on fully dense Ti c.p. and TiNbTa: in the alloy, the cell shows a more differentiated phenotype with extracellular matrix secretion (Figure 7).

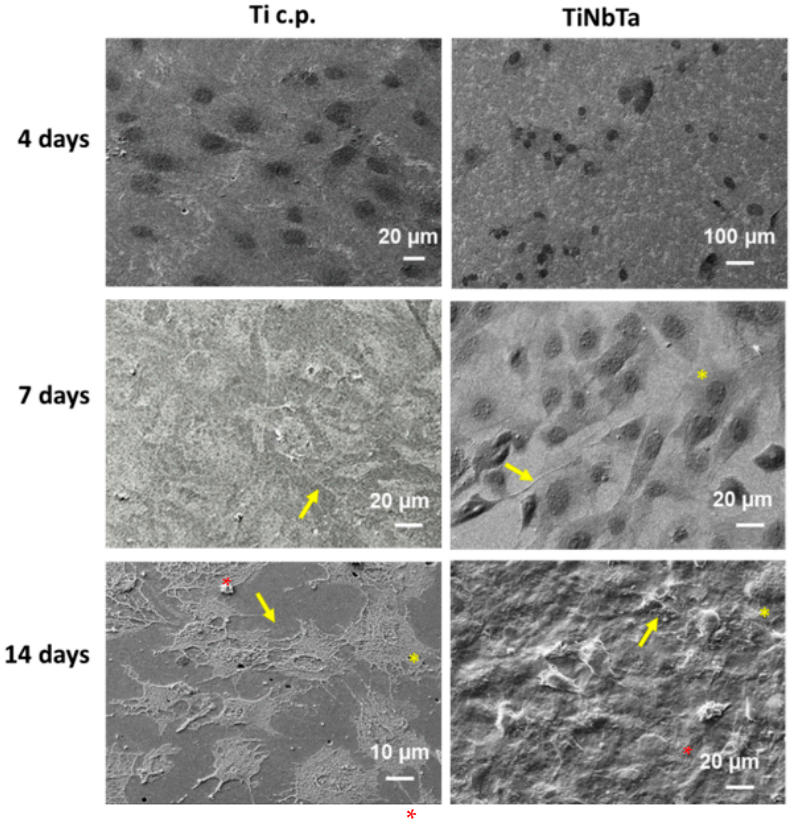

Figure 7. SEM micrographs at 4, 7, and 14 days of osteoblast culture growing on fully dense Ti c.p. or TiNbTa surface. Cell morphology and osteoblast proliferation are observed with filopodia marked by yellow arrows and lamellipodia indicated by yellow asterisks (flattened extension of a cell, by which it adheres to a surface) . The small hexagonal-structure vesicles are indicated by a red asterisk, which suggests hydroxyapatite on the cell surface.

From day 7, the cells present a more differentiated phenotype as observed in the SEM images, and the ALP activity decreases. These results confirm those published by Lin-Jie Li et al. in which they observed that, on smooth surfaces, cells exhibited a high proliferation rate; however, the levels of alkaline phosphatase and osteocalcin were low, which suggests a phenotypic change in differentiated osteoblasts [40,44]. In another interesting study, Sungsin Jo et al. [45] observed a delay in the mineralization and differentiation of osteoblastic cells following the elimination of the ALP gene, thereby demonstrating that higher levels of the enzyme are necessary to promote the initiation of differentiation in osteoblasts.

In summary, these results show that the TiNbTa alloy has a good growth capacity and a low elastic modulus, and therefore this material should be considered as a good candidate for use in the biomedical area. However, complementary and in vivo, biological tests

remain necessary to fully understand how the TiNbTa alloy affects the osseointegration process and how its use in biomedical applications could be improved.

4. Conclusions

A TiNbTa potential prosthetic biomaterial is developed and evaluated, and its biocompatibility is compared with the current Ti c.p. used as a bone-replacement implant material. The main conclusions obtained can be set out as follows:

- It is possible to obtain a similar Young's modulus and higher yield strength than those of the cortical bone tissue through the development of TiNbTa foams and Ti c.p. foams. These interesting properties are even better for the TiNbTa foams in comparison with the Ti c.p. foams;
- In particular, regarding the σy/E index, the TiNbTa_20 and TiNbTa_30, corresponding to TiNbTa foams with volumetric porosity values of 20 and 30%, respectively, appear to present the optimal potential prosthetic biomaterials for cortical bone replacements (higher index). They also displayed interesting values of E = 25.5 GPa and 17.7 GPa, and σy = 976 Mpa and 685 MPa, respectively. In addition, the high yield strengths help to prevent any plastic deformation for a hypothetical implant fabricated by this material;
- In turn, the mechanical behavior for cancellous bone tissue (E less than 1 GPa and σy = 9 MPa) could also be reached by the TiNbTa foams with an 80 volumetric percentage of porosity (E = 1 GPa and σy = 40 MPa), However, the high porosity makes its manufacture less feasible;
- In vitro tests show the successful adhesion, proliferation, and differentiation of osteoblasts (MC3T3 cell line), thereby confirming the biocompatibility and non-toxicity of TiNbTa samples;
- On the other hand, osteoblasts cultured in the TiNbTa samples showed the same metabolic and alkaline phosphate activity as those cultured in the Ti c.p. samples. Therefore, TiNbTa samples show a bio-functional behavior balance, which promotes in vitro osseointegration and solves the stress-shielding phenomenon.

Author Contributions: Conceptualization, project administration, supervision, methodology, M.G., M.J.M.-G., E.C. and Y.T.; investigation A.d.F.C., L.S., M.Á.V.-G. and C.G.-G.; formal analysis, M.A.C. and F.J.O.-M. validation, M.G. and E.C.; discussion and writing—original draft preparation, all the authors. All authors have read and agreed to the published version of the manuscript.

Funding: This work was supported by the Ministry of Science and Innovation of Spain under the grant PID2019-109371GB-I00 and by the Junta de Andalucía—FEDER (Spain) through the Project Ref. US-1259771.

Institutional Review Board Statement: Not applicable.

Informed Consent Statement: Not applicable.

Data Availability Statement: The data presented in this study are available on request from the corresponding author. The data are not publicly available due to privacy.

Conflicts of Interest: Authors declare no conflict of interest.

References

1. Holzapfel, B.M.; Reichert, J.C.; Schantz, J.-T.; Gbureck, U.; Rackwitz, L.; Nöth, U.; Jakob, F.; Rudert, M.; Groll, J.; Hutmacher, D.W. How smart do biomaterials need to be? A translational science and clinical point of view. *Adv. Drug Deliv. Rev.* **2013**, *65*, 581–603. [CrossRef] [PubMed]
2. Li, Y.; Yang, C.; Zhao, H.; Qu, S.; Li, X.; Li, Y. New developments of ti-based alloys for biomedical applications. *Materials* **2014**, *7*, 1709–1800. [CrossRef] [PubMed]
3. Geetha, M.; Singh, A.K.; Asokamani, R.; Gogia, A.K. Ti based biomaterials, the ultimate choice for orthopaedic implants—A review. *Prog. Mater. Sci.* **2009**, *54*, 397–425. [CrossRef]
4. Zhang, L.C.; Chen, L.Y. A Review on Biomedical Titanium Alloys: Recent Progress and Prospect. *Adv. Eng. Mater.* **2019**, *21*, 1801215. [CrossRef]

5. Rho, J.Y.; Ashman, R.B.; Turner, C.H. Young's modulus of trabecular and cortical bone material: Ultrasonic and microtensile measurements. *J. Biomech.* **1993**, *26*, 111–119. [CrossRef]
6. Muñoz, S.; Castillo, S.M.; Torres, Y. Different models for simulation of mechanical behaviour of porous materials. *J. Mech. Behav. Biomed. Mater.* **2018**, *80*, 88–96. [CrossRef]
7. Kourtis, S.; Damanaki, M.; Kaitatzidou, S.; Kaitatzidou, A.; Roussou, V. Loosening of the fixing screw in single implant crowns: Predisposing factors, prevention and treatment options. *J. Esthet. Restor. Dent.* **2017**, *29*, 233–246. [CrossRef]
8. Trueba, P.; Chicardi, E.; Rodríguez-Ortiz, J.A.; Torres, Y. Development and implementation of a sequential compaction device to obtain radial graded porosity cylinders. *J. Manuf. Process.* **2020**, *50*, 142–153. [CrossRef]
9. Wang, X.; Xu, S.; Zhou, S.; Xu, W.; Leary, M.; Choong, P.; Qian, M.; Brandt, M.; Xie, Y.M. Topological design and additive manufacturing of porous metals for bone scaffolds and orthopaedic implants: A review. *Biomaterials* **2016**, *83*, 127–141. [CrossRef]
10. Zhou, L.; Yuan, T.; Tang, J.; He, J.; Li, R. Mechanical and corrosion behavior of titanium alloys additively manufactured by selective laser melting—A comparison between nearly β titanium, α titanium and α + β titanium. *Opt. Laser Technol.* **2019**, *119*, 105625. [CrossRef]
11. Pilliar, R.M. Metallic biomaterials. In *Biomedical Materials*; Springer: Boston, MA, USA, 2009; pp. 41–81.
12. Abdel-Hady Gepreel, M.; Niinomi, M. Biocompatibility of Ti-alloys for long-term implantation. *J. Mech. Behav. Biomed. Mater.* **2013**, *20*, 407–415. [CrossRef] [PubMed]
13. Biesiekierski, A.; Wang, J.; Abdel-Hady Gepreel, M.; Wen, C. A new look at biomedical Ti-based shape memory alloys. *Acta Biomater.* **2012**, *8*, 1661–1669. [CrossRef]
14. Cui, C.; Hu, B.M.; Zhao, L.; Liu, S. Titanium alloy production technology, market prospects and industry development. *Mater. Des.* **2010**, *32*, 1684–1691. [CrossRef]
15. Kim, E.S.; Jeong, Y.H.; Choe, H.C.; Brantley, W.A. Formation of titanium dioxide nanotubes on Ti-30Nb-xTa alloys by anodizing. *Thin Solid Film.* **2013**, *549*, 141–146. [CrossRef]
16. Schmidt, R.; Pilz, S.; Lindemann, I.; Damm, C.; Hufenbach, J.; Helth, A.; Geissler, D.; Henss, A.; Rohnke, M.; Calin, M.; et al. Powder metallurgical processing of low modulus β-type Ti-45Nb to bulk and macro-porous compacts. *Powder Technol.* **2017**, *322*, 393–401. [CrossRef]
17. Chicardi, E.; Aguilar, C.; Sayagués, M.J.; García-Garrido, C. Influence of the Mn content on the TiNbxMn alloys with a novel fcc structure. *J. Alloys Compd.* **2018**, *746*, 601–610. [CrossRef]
18. Shen, X.; Zhang, Y.; Jiang, Y.; Zhou, R. Corrosion behavior of Ti-35Nb-7Zr-5Ta alloy prepared by spark plasma sintering in Hank's artificial body fluid. *Corros. Sci. Prot. Technol.* **2016**, *28*, 543–548.
19. Stráský, J.; Harcuba, P.; Václavová, K.; Horváth, K.; Landa, M.; Srba, O.; Janeček, M. Increasing strength of a biomedical Ti-Nb-Ta-Zr alloy by alloying with Fe, Si and O. *J. Mech. Behav. Biomed. Mater.* **2017**, *71*, 329–336. [CrossRef]
20. Liu, Q.; Meng, Q.; Guo, S.; Zhao, X. α′ Type Ti–Nb–Zr alloys with ultra-low Young's modulus and high strength. *Prog. Nat. Sci. Mater. Int.* **2013**, *23*, 562–565. [CrossRef]
21. Zhentao, Y.; Lian, Z. Influence of martensitic transformation on mechanical compatibility of biomedical β type titanium alloy TLM. *Mater. Sci. Eng. A* **2006**, *438–440*, 391–394. [CrossRef]
22. Jawed, S.F.; Rabadia, C.D.; Liu, Y.J.; Wang, L.Q.; Li, Y.H.; Zhang, X.H.; Zhang, L.C. Mechanical characterization and deformation behavior of β-stabilized Ti-Nb-Sn-Cr alloys. *J. Alloys Compd.* **2019**, *792*, 684–693. [CrossRef]
23. Jawed, S.F.; Rabadia, C.D.; Liu, Y.J.; Wang, L.Q.; Li, Y.H.; Zhang, X.H.; Zhang, L.C. Beta-type Ti-Nb-Zr-Cr alloys with large plasticity and significant strain hardening. *Mater. Des.* **2019**, *181*, 108064. [CrossRef]
24. Samuel, S.; Nag, S.; Nasrazadani, S.; Ukirde, V.; El Bouanani, M.; Mohandas, A.; Nguyen, K.; Banerjee, R. Corrosion resistance and in vitro response of laser-deposited Ti-Nb-Zr-Ta alloys for orthopedic implant applications. *J. Biomed. Mater. Res.* **2010**, *94*, 1251–1256. [CrossRef] [PubMed]
25. Kaur, M.; Singh, K. Review on titanium and titanium-based alloys as biomaterials for orthopaedic applications. *Mater. Sci. Eng. C* **2019**, *102*, 844–862. [CrossRef] [PubMed]
26. Chicardi, E.; Gutiérrez-González, C.F.; Sayagués, M.J.; García-Garrido, C. Development of a novel TiNbTa material potentially suitable for bone replacement implants. *Mater. Des.* **2018**, *145*, 88–96. [CrossRef]
27. García-Garrido, C.; Gutiérrez-González, C.; Torrecillas, R.; Pérez-Pozo, L.; Salvo, C.; Chicardi, E. Manufacturing optimisation of an original nanostructured (beta + gamma)-TiNbTa material. *J. Mater. Res. Technol.* **2019**, *8*, 2573–2585. [CrossRef]
28. Hussein, A.H.; Gepreel, M.A.H.; Gouda, M.K.; Hefnawy, A.M.; Kandil, S.H. Biocompatibility of new Ti-Nb-Ta base alloys. *Mater. Sci. Eng. C* **2016**, *61*, 574–578. [CrossRef]
29. Mondal, D.P.; Ramakrishnan, N.; Suresh, K.S.; Das, S. On the moduli of closed-cell aluminum foam. *Scr. Mater.* **2007**, *57*, 929–932. [CrossRef]
30. Zhang, L.C.; Klemm, D.; Eckert, J.; Hao, Y.L.; Sercombre, T.B. Manufacture by selective laser melting and mechanical behavior of a biomedical Ti–24Nb–4Zr–8Sn alloy. *Scr. Mater.* **2011**, *65*, 21–24. [CrossRef]
31. Currey, J.D. Bone and Natural Composites: Properties. In *Encyclopedia of Materials: Science and Technology*; Elsevier: Amsterdam, The Netherlands, 2001; pp. 776–781.
32. Donato, T.A.; de Almeida, L.H.; Nogueira, R.A.; Niemeyer, T.C.; Grandini, C.R.; Caram, R.; Schneider, S.G.; Santos, A.R., Jr. Cytotoxicity study of some Ti alloys used as biomaterial. *Mater. Sci. Eng. C* **2009**, *29*, 1365–1369. [CrossRef]

33. Cremasco, A.; Messias, A.D.; Esposito, A.R.; Duek, E.A.D.R.; Caram, R. Effects of alloying elements on the cytotoxic response of titanium alloys. *Mater. Sci. Eng. C* **2011**, *31*, 833–839. [CrossRef]
34. Wang, Y.B.; Zheng, Y.F. Corrosion behaviour and biocompatibility evaluation of low modulus Ti-16Nb shape memory alloy as potential biomaterial. *Mater. Lett.* **2009**, *63*, 1293–1295. [CrossRef]
35. Li, Y.; Wong, C.; Xiong, J.; Hodgson, P.; Wen, C. Cytotoxicity of titanium and titanium alloying elements. *J. Dent. Res.* **2010**, *89*, 493–497. [CrossRef] [PubMed]
36. Okazaki, Y.; Gotoh, E. Comparison of metal release from various metallic biomaterials in vitro. *Biomaterials* **2005**, *26*, 11–21. [CrossRef]
37. Lamolle, S.F.; Monjo, M.; Lyngstadaas, S.P.; Ellingsen, J.E.; Haugen, H.J. Titanium implant surface modification by cathodic reduction in hydrofluoric acid: Surface characterization and in vivo performance. *J. Biomed. Mater. Res.-Part A* **2009**, *88*, 581–588. [CrossRef]
38. Wang, Q.; Zhang, H.; Li, Q.; Ye, L.; Gan, H.; Liu, Y.; Wang, H.; Wang, Z. Biocompatibility and osteogenic properties of porous tantalum. *Exp. Ther. Med.* **2015**, *9*, 780–786. [CrossRef]
39. Shimko, D.A.; Shimko, V.F.; Sander, E.A.; Dickson, K.F.; Nauman, E.A. Effect of porosity on the fluid flow characteristics and mechanical properties of tantalum scaffolds. *J. Biomed. Mater. Res.-Part B Appl. Biomater.* **2005**, *73*, 315–324. [CrossRef]
40. Li, L.J.; Kim, S.N.; Cho, S.A. Comparison of alkaline phosphatase activity of MC3T3-E1 cells cultured on different Ti surfaces: Modified sandblasted with large grit and acid-etched (MSLA), laser-treated, and laser and acid-treated Ti surfaces. *J. Adv. Prosthodont.* **2016**, *8*, 235–240. [CrossRef]
41. Owen, T.A.; Aronow, M.; Shalhoub, V.; Barone, L.M.; Wilming, L.; Tassinari, M.S.; Kennedy, M.B.; Pockwinse, S.; Lian, J.B.; Stein, G.S. Progressive development of the rat osteoblast phenotype in vitro: Reciprocal relationships in expression of genes associated with osteoblast proliferation and differentiation during formation of the bone extracellular matrix. *J. Cell. Physiol.* **1990**, *143*, 420–430. [CrossRef]
42. Siddiqui, J.A.; Swarnkar, G.; Sharan, K.; Chakravarti, B.; Sharma, G.; Rawat, P.; Kumar, M.; Khan, F.M.; Pierroz, D.; Maurya, R.; et al. 8,8″-Biapigeninyl stimulates osteoblast functions and inhibits osteoclast and adipocyte functions: Osteoprotective action of 8,8″-biapigeninyl in ovariectomized mice. *Mol. Cell. Endocrinol.* **2010**, *323*, 256–267. [CrossRef] [PubMed]
43. Martín González, A.; Allo Miguel, G.; Aramendi Ramos, M.; Librizzi, S.; Jiménez, C.; Hawkins, F.; Martínez Díaz-Guerra, G. Different development of serum sclerostin compared to other bone remodeling markers in the first year after a liver transplant. *Rev. Osteoporos. Metab. Miner.* **2019**, *11*, 25–29. [CrossRef]
44. Boyan, B.D.; Hummert, T.W.; Dean, D.D.; Schwartz, Z. Role of material surfaces in regulating bone and cartilage cell response. *Biomaterials* **1996**, *17*, 137–146. [CrossRef]
45. Jo, S.; Han, J.; Lee, Y.L.; Yoon, S.; Lee, J.; Wang, S.E.; Kim, T.H. Regulation of osteoblasts by alkaline phosphatase in ankylosing spondylitis. *Int. J. Rheum. Dis.* **2019**, *22*, 252–261. [CrossRef] [PubMed]